Magnetic Doublon Bound States in the Kondo Lattice Model

Roman Rausch,[1,*] Michael Potthoff,[2] and Norio Kawakami[1]
[1]Department of Physics, Kyoto University, Kyoto 606-8502, Japan
[2]Department of Physics, University of Hamburg, Jungiusstraße 9, D-20355 Hamburg, Germany

(Received 25 September 2019; published 18 November 2019)

We present a novel pairing mechanism for electrons, mediated by magnons. These paired bound states are termed "magnetic doublons." Applying numerically exact techniques (full diagonalization and the density-matrix renormalization group, DMRG) to the Kondo lattice model at strong exchange coupling J for different fillings and magnetic configurations, we demonstrate that magnetic doublon excitations exist as composite objects with very weak dispersion. They are highly stable, support a novel "inverse" colossal magnetoresistance and potentially other effects.

DOI: 10.1103/PhysRevLett.123.216401

Motivation.—The Mott-insulating state of the single-band Hubbard model, driven by repulsive Coulomb interaction, remains an enduring paradigm in strongly correlated electron physics. An excitation of electrons across the Mott gap to the upper Hubbard band forms "doublons," quasiparticles which are stabilized by the strong Hubbard interaction U and which persist as bound states on a timescale growing exponentially with U [1,2]. This stability provides a bottleneck in the relaxation dynamics [3], and several propositions have been made to exploit this effect. (i) Since doublons effectively behave as hard-core bosons with an attractive interaction, the creation of a metastable superfluid state is conceivable. Being an excited state far from equilibrium, however, such a state has to be engineered in an optical lattice [4] or by photodoping [5]. (ii) The stability of doublons on a long timescale makes Mott insulators candidate materials for solar cells [6,7]. In this case, incident light creates a doublon-hole excitation which quickly recombines if there is no interaction, leading to merely diffusive charge separation. With interaction, on the other hand, a stable doublon is created that can be separated from the hole more efficiently. (iii) The so-called "quantum distillation" is a cooling method for atoms in optical lattices [8–10]. Having trapped a number of doublons and then releasing the trap, one observes that while fast components of the block escape, the rest bunches together, leading to an increase of the local double occupancy and hence to an approximate band insulator with low entropy.

Here, we demonstrate the existence of a novel quasiparticle, the "magnetic doublon." Opposed to the conventional one, it is stabilized by magnetic degrees of freedom rather than by a strong Hubbard U. The magnetic doublon is in fact a bound state of a conventional doublon and a magnon. It requires a magnetic background and consists of a double occupancy in the vicinity of a spin-flip excitation, thus being a quasiparticle that is itself formed out of two quasiparticles.

We will argue that the Kondo lattice model (KLM) is the most simple system that hosts the magnetic doublon. Key to an understanding of the binding mechanism is the limit of a strong local exchange coupling J. This regime is of high relevance for materials like doped manganites [11,12] and is precisely the limit accessible in the simulation of the KLM by an ultracold ^{173}Yb gas in an optical lattice [13]. As the concept is fairly general, one should expect magnetic doublons in other contexts as well, e.g., in multi-orbital, strong-J systems, such as Hund's metals [14]. The magnetic doublon provides an alternative route to the same functionalities (i)–(iii) of the conventional doublon but in addition to that also has a couple of further intriguing properties as will be shown here.

Two-electron exact solution.—The quintessence of the magnetic doublon concept can be already understood in the two-electron case ($N = 2$). We consider a one-dimensional lattice with periodic boundaries; this is convenient methodically, but not essential. The KLM Hamiltonian reads

$$H = -T\sum_{\langle ij\rangle\sigma}(c^\dagger_{i\sigma}c_{j\sigma} + \text{H.c.}) + J\sum_i \mathbf{S}_i \cdot \mathbf{s}_i. \qquad (1)$$

Here, $c^\dagger_{i\sigma}$ creates an electron with the spin projection $\sigma = \uparrow, \downarrow$ at site i. Furthermore, $\mathbf{s}_i = \sum_{\sigma\sigma'} c^\dagger_{i\sigma}\boldsymbol{\tau}_{\sigma\sigma'}c_{i\sigma'}/2$ (with the Pauli matrices $\boldsymbol{\tau}$) is the spin of the electron at site i and $\mathbf{S}_i$ is the local spin with quantum number $1/2$. $J > 0$ denotes the antiferromagnetic (AFM) exchange interaction. The hopping amplitude $T \equiv 1$ between nearest neighbors (denoted by the angle brackets $\langle ij\rangle$) fixes the energy and time units ($\hbar \equiv 1$). The ground state of the model in the strong-J regime on L sites is ferromagnetic (FM) with total spin $S = (L - N)/2$, for $N = 1, 2, \ldots, L - 1$ and becomes a singlet $S = 0$ at half filling $N = L$ [15].

For $N = 2$ electrons, i.e., at most one doublon, we can develop a "doublon band theory" [16]. Effective doublon-doublon interactions show up at higher fillings; this is discussed later. We perform full diagonalization to simultaneously get the many-body eigenstates of H, the particle-number operator $\hat{N}$, the squared total spin operator $\mathbf{S}_{\mathrm{tot}}^2 = [\sum_i (\mathbf{S}_i + \mathbf{s}_i)]^2$, and the total momentum operator $\hat{P}$ (derived in Ref. [17]), with the corresponding quantum numbers E, $N = 2$, $S(S+1)$, and K, respectively. Several spin symmetry sectors are possible: $S = (L+2)/2$ yields the trivial fully polarized case where the spin exchange $\propto J$ is inactive. $S = L/2$, i.e., one spin flip away from full polarization is discussed in the Supplemental Material [18]. Here, we focus on the case $S = (L-2)/2$ (two spin flips), as this sector also contains the ground state.

Figure 1 displays the results. Four types of states can be distinguished by calculating the average local spin correlation per electron $\langle \mathbf{S} \cdot \mathbf{s} \rangle_{\mathrm{loc}}/N \equiv \sum_i \langle \mathbf{S}_i \cdot \mathbf{s}_i \rangle / N$ and the total double occupancy $\langle n^d \rangle \equiv \sum_i \langle n_{i\uparrow} n_{i\downarrow} \rangle$. In the lowest-energy states (labeled $P+P$), the electrons are almost completely AFM correlated with the localized spins, so that $\langle \mathbf{S} \cdot \mathbf{s} \rangle_{\mathrm{loc}}/2 \approx -3/4$. This causes a fully polarized local-spin system to be favorable because the "kinetic" term $\propto T$ of H is minimized. For one electron, this limit of a "magnetic polaron" has been amply investigated in the past [19–21]. If one of the polarons decays into an FM-aligned electron and a magnon, we get $\langle \mathbf{S} \cdot \mathbf{s} \rangle_{\mathrm{loc}}/2 \approx (-3/4 + 1/4)/2 = -1/4$ (labeled $P+S$). If both polarons decay, we get the ferromagnetic correlation $\langle \mathbf{S} \cdot \mathbf{s} \rangle_{\mathrm{loc}}/2 \approx +1/4$ (labeled $S+S$). However, in between these two scattering "continua," around $E = 0$, one finds solutions with $\langle \mathbf{S} \cdot \mathbf{s} \rangle_{\mathrm{loc}}/2 \approx 0$ and $\langle n^d \rangle \approx 1$, which can thus be identified as doublon states (labeled D). We note that switching the sign of J from AFM to FM simply exchanges the scattering with the polaron part, but does not affect the presence of the doublon in between.

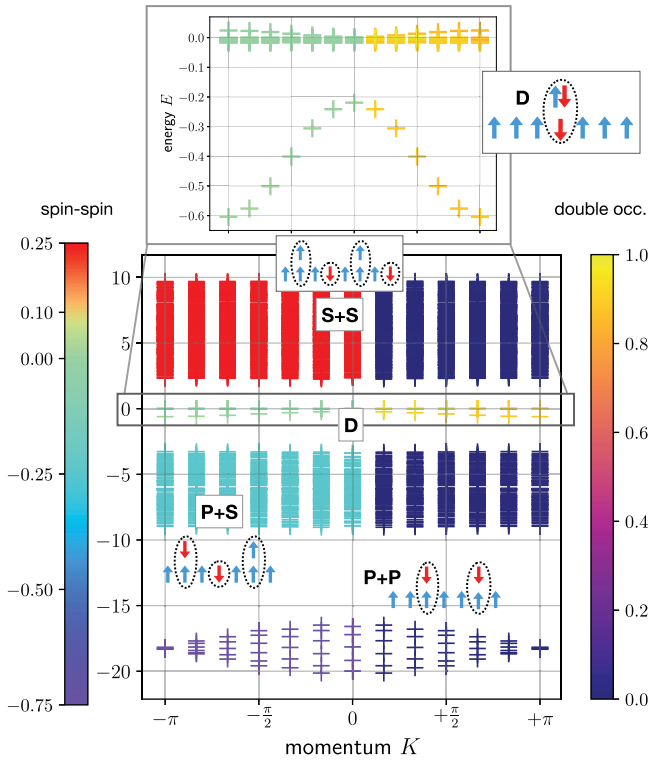

FIG. 1. Many-body eigenenergies as a function of the total momentum K of the one-dimensional KLM with $L = 12$ sites at $J = 12$. Each cross refers to an eigenstate in the sector $N = 2$, $S = (L-N)/2$. The plot is symmetric to $K = 0$. Color code (for $K \leq 0$, left) gives the local spin-spin correlation per electron $\sum_i \langle \mathbf{S}_i \cdot \mathbf{s}_i \rangle / N$, and (for $K > 0$, right) the double occupancy $\sum_i \langle n_{i\uparrow} n_{i\downarrow} \rangle$. From lowest to highest energy, the states are $P+P$, two polarons; $P+S$, polaron and scattered electron; D, magnetic doublon; $S+S$, two scattered electrons. The doublon bands are magnified in the upper part.

Magnetic doublon.—Now, zooming into the doublon states (topmost panel of Fig. 1), we discover that there are in fact two distinct features with a small gap in between, a narrow and a broad one. The narrow one is expected to form a continuum of states in the $L \to \infty$ limit. Varying J, we find that its bandwidth scales as $W \sim J^{-3}$ for strong J (see Fig. 2). The magnetic doublon corresponds to the broad structure composed of L eigenstates. Its dispersion has minima at $K = \pm\pi$ and the bandwidth scales as $W \sim J^{-1}$ (Fig. 2).

It is possible to analytically derive a first-order effective model that projects onto the states of the broad doublon band by using T/J as a small parameter and neglecting single occupancy (which is essentially the Schrieffer-Wolff

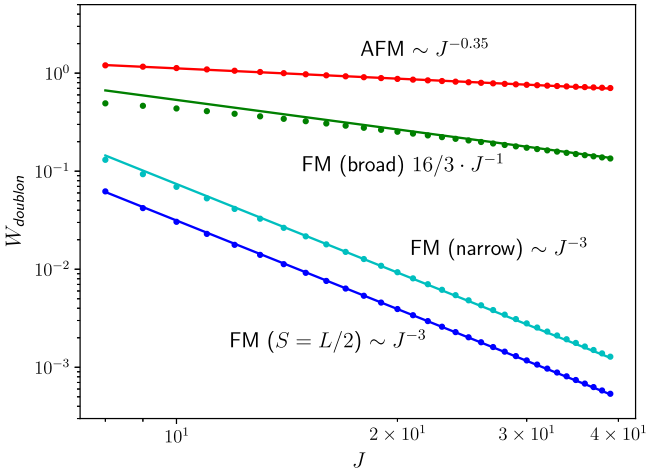

FIG. 2. Points: Doublon bandwidth as obtained by full diagonalization for various cases. (i) $S = (L-2)/2$, FM ground state ($L = 12$); for broad and narrow dispersions see text. (ii) $S = L/2$, FM ground state ($L = 16$), see Ref. [18]. (iii) $S = 0$, AFM ground state ($L = 8$), see text. Lines: Fits $W = \mathrm{const} \times J^{-r}$ as indicated, except for the broad doublon bandwidth which is taken from the effective model Eq. (2).

transformation, cf. Refs. [4,20,22] and Ref. [18]). We obtain the following result:

$$H_{\rm eff} = J'_K \sum_{\langle ij \rangle} (d_i^\dagger d_j + d_j^\dagger d_i - 2 n_i^d n_j^d + n_i^d + n_j^d) \cdot (\mathbf{S}_i \cdot \mathbf{S}_j - 1/4). \quad (2)$$

Here, $d_i^\dagger = c_{i\downarrow}^\dagger c_{i\uparrow}^\dagger$ creates a double occupancy at site i, now a hard-core boson (with $[d_i, d_j^\dagger] = \delta_{ij}$ and $d_i^{\dagger 2} = 0$). The corresponding density is $n_i^d = d_i^\dagger d_i$. As compared to the related expression for the Hubbard model [4], we find a different hopping amplitude $J'_K = 8T^2/3J$ (rather than $2T^2/U$) and, more importantly, an interaction with the magnetic substrate, given by the spin-spin product in Eq. (2). Thereby, the sign of the doublon-doublon interaction becomes dependent on the nature of the magnetic ground state. It is attractive in the ferro- and repulsive in the antiferromagnetic case.

It is instructive to employ the transformation $d_i^\dagger = (-1)^i T_i^+$, $n_i^d = T_i^z + 1/2$ from hard-core bosons to pseudospin operators $\boldsymbol{T}_i$, which fulfill the usual spin commutation relations. We obtain a rather compact spin-pseudospin model:

$$H_{\rm eff} = -2J'_K \sum_{\langle ij \rangle} (\mathbf{T}_i \cdot \mathbf{T}_j - 1/4) \cdot (\mathbf{S}_i \cdot \mathbf{S}_j - 1/4), \quad (3)$$

which is manifestly invariant under the spin- and charge-SU(2) symmetries of the system [23,24].

Note the following important consequence: In the effective model, the subspace $S = (L-2)/2$ contains one doublon and one magnon (the number of states is L^2), and $H_{\rm eff}$ only gives a nonzero result if they are at least nearest neighbors. The delocalization of L of these bound states thus forms the "broad" dispersion of the magnetic doublon band, while the remaining ones have zero energy.

Numerical evidence shows that the degeneracy of the remaining states is lifted in third order, see Fig. 2, resulting in a narrow continuum where a doublon and a magnon are propagating independently through the lattice. A scaling of the bandwidth $\sim J^{-3}$ is also seen in the results for the $S = L/2$ sector; see the Supplemental Material [18] and Fig. 2. For $S = L/2$, the phase space is highly restricted and one can either have a doublon or a magnon, but not both. Still, the doublon can delocalize in a higher-order process by creating and absorbing a virtual magnon. We suspect that the same mechanism is at work for the narrow doublon band of Fig. 1.

Inverse CMR effect.—The broad bandwidth of the magnetic doublon is strongly dependent on the underlying magnetic configuration. This is demonstrated in Fig. 2 where it is compared with the bandwidth for the case of an antiferromagnetic singlet ($S = 0$). Such a ground state can easily be stabilized by adding a weak direct coupling $J_{\rm dir} \sum_{\langle ij \rangle} \mathbf{S}_i \cdot \mathbf{S}_j$ to the Hamiltonian ($J_{\rm dir} = 0.1$). We find the same four types of states, but the magnetic doublon bandwidth now scales as $W \sim J^{-0.35}$. Hence, the magnetic doublon has a substantially broader dispersion if the spin system is not polarized homogeneously. This is intuitively clear, as it requires a bound magnon to propagate, and the antiferromagnet (but also a disordered local-moment paramagnetic state) provides a much larger phase space in terms of spin flips to assist the propagation. We note that as compared with the conventional colossal magnetoresistance (CMR) effect, transport is alleviated by spin disorder rather than impeded. Hence, there is an "inverse" CMR effect in controlling the nonequilibrium transport properties of magnetic doublons via temperature or magnetic switching.

Electron spectroscopy at finite filling ratio.—In principle, the most direct access to observing magnetic doublon excitations is given by appearance-potential spectroscopy [25,26], where there are two additional electrons in the final state, predominantly created at the same site. This is shown in the Supplemental Material [18]. Here, we instead focus on k-resolved single-electron spectroscopy, which is a widely established experimental technique. For convenience we will consider electron addition, i.e., the inverse photoemission spectrum from systems with low band filling. This is related to standard photoemission (one-electron removal) at high band fillings via particle-hole symmetry.

We demonstrate that the magnetic doublon can be seen as a satellite for a finite filling $n = N/L$ in the thermodynamic limit (large N, large L). This is shown in Fig. 3, which displays the spin-resolved spectrum at $n = 1/4$ (one-eighth filling), given by

$$A_\sigma(k,\omega) = \langle 0 | c_{k\sigma} \delta(\omega + E_0 - H) c_{k\sigma}^\dagger | 0 \rangle, \quad (4)$$

where $c_{k\sigma} = \sum_i e^{-ikR_i} c_{i\sigma}/\sqrt{L}$, and where $|0\rangle$ is the N-particle ground state with magnetization M, which is the eigenvalue of $\sum_i (S_i^z + s_i^z)$. Note that the spin-$\uparrow$ spectrum has been rigidly shifted to align with the spin-$\downarrow$ spectrum for better comparison. In the latter case, $\omega = 0$ refers to the Fermi edge.

To calculate the spectral function, we have used a density-matrix renormalization group (DMRG) code which actually exploits the full SU(2) spin symmetry along with the U(1) charge symmetry of the model, combined with the Chebyshev polynomial technique [16,27]. As before, we control the total spin S, but are able to resolve the result according to M in a postprocessing step from a single calculation.

In the spin-down (minority) case, the lowest-frequency states are given by processes where the added electron forms a polaron with the magnetic substrate. In the strong-coupling limit, we can think of the ground state as being filled by noninteracting polarons which occupy the

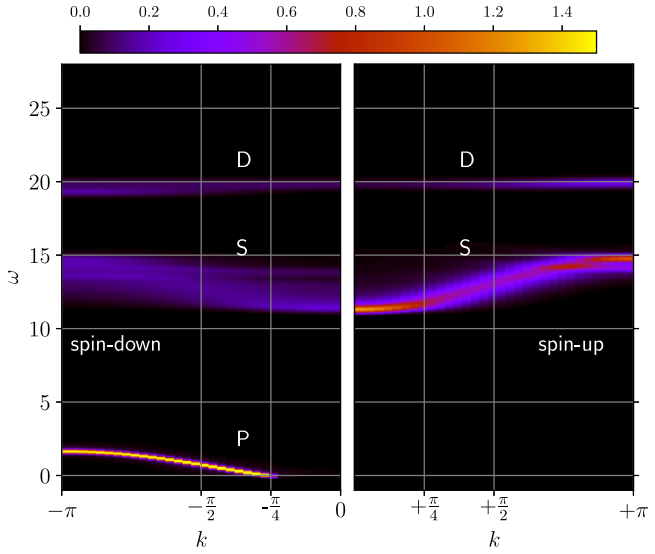

FIG. 3. Inverse photoemission spectrum Eq. (4) as obtained by Chebyshev-expansion DMRG for $n = 1/4$ ($N = 16$, $L = 64$), $S = (L - N)/2$ and $J = 12$. Left: spin-down (minority). Right: spin-up (majority, shifted rigidly by $\Delta\omega \approx 11.2$ to align with the spin-down spectrum). Both spectra are symmetric with respect to $k = 0$. P, polaron; S, scattered state; D, doublon.

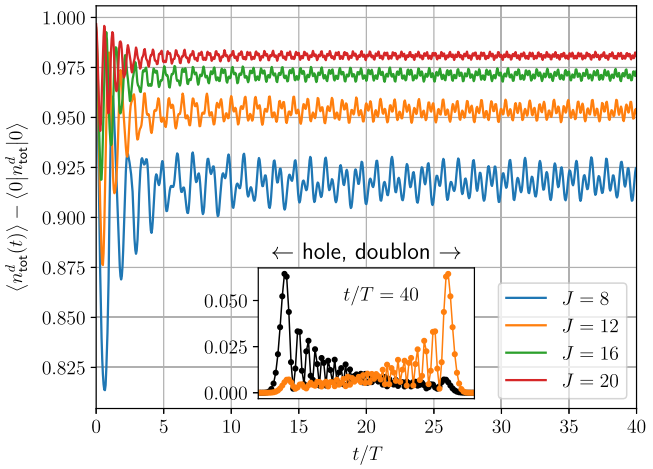

FIG. 4. Time dependence of the total double occupancy (with ground-state value subtracted) after a doublon-hole excitation as obtained for an infinite MPS with $S = 0$, $n = 1$ on a heterogeneous section of $L = 100$ lattice sites. Inset: real-space snapshot at time $t/T = 40$ of the double occupancy (orange, propagating to the right) and the empty occupancy (black, propagating to the left) for $J = 12$.

lowest-momenta states, so that the dispersion of the excitation ("P") starts at $k \approx n\pi = \pi/4$ for $\omega = 0$. Flipping the incident electron spin then leads to a higher scattering state ("S"), but there is also some probability to find another electron with which a doublon state can be formed ("D"). In the spin-up (majority) case, the electron has a high probability to find empty sites (because of the low density n), upon which it propagates with a free dispersion of bandwidth $W = 4T$ (S). However, there is again some probability to form a doublon with an electron from the ground state (D). In both cases, the energy distance of the doublon to the scattering states is about $J/2$ and to the lowest polaron states about $3J/2$, consistent with the two-electron eigenstates of Fig. 1. The doublon excitation (D) has an extremely weak dispersion and is basically spin independent. We did not attempt to resolve its internal structure, i.e., the bound magnetic doublon and the narrow continuum.

Real-time dynamics.—Finally, we demonstrate the stability of magnetic doublons. To this end a local doublon-hole excitation is created suddenly at $t = 0$ by applying the correlated-hopping operator $C_{i,i+1} = \sum_\sigma (1 - n_{i,-\sigma}) c_{i\sigma} c^\dagger_{i+1}$, $\sigma n_{i+1,-\sigma}$ locally to the ground state, i.e., $|\Psi(0)\rangle = C_{i,i+1}|0\rangle$ Then this state is propagated in time, $|\Psi(t)\rangle = \exp(-iHt)|\Psi(0)\rangle$, and the total double occupancy $\langle n^d_{\rm tot}(t)\rangle = \sum_i \langle \Psi(t)|n^d_i|\Psi(t)\rangle$ is measured at each step. Apart from being a general study of doublon decay in real time, this setup could also be regarded as a crude modeling of the effect of an incident photon [6]. It is advantageous to use a correlated-hopping operator instead of just $c_{i\sigma} c^\dagger_{i+1,\sigma}$, as this ensures that the double occupancy will be zero on site i and one on site $i + 1$ independently of the initial configuration. We furthermore subtract the ground-state contribution of $\langle n^d_{\rm tot}\rangle$ to facilitate the comparison for different values of J. Since the largest cross section for this excitation is found at half filling, we consider the AFM singlet state ($S = 0$) at $n = 1$. We first calculate the ground state of an infinite system using the variational uniform matrix-product states (VUMPS) algorithm [28] with SU(2) spin and U(1) charge symmetry; then a heterogeneous section [29] is assembled where the excitation is allowed to spread [30].

We find that the magnetic doublon picture continues to hold in this regime, even as the many-body effects are strongest. Figure 4 shows that, after a few inverse hoppings, the double occupancy settles at a constant plateau quite close to the initial value of (almost) unity without any further decay on the accessible time scale. The larger J, the closer it stays to unity. As compared to doublon dynamics in the Hubbard model [6,31,32], there are important differences resulting from the different binding mechanisms: A Fourier analysis (not shown) indicates that there are two dominating oscillation frequencies in the Kondo case, which are roughly given by $J/2$ and $3J/2$. Furthermore, in the Hubbard case the maximal velocity of the wave front is basically given by the Fermi velocity $v_{\rm max} \approx 2T$, while in the Kondo case we find $v_{\rm max} \approx T$, which in fact corresponds to the polaron velocity in the strong-J limit [20]. Thus, qualitatively, a propagating doublon excitation of an antiferromagnetic Mott insulator should be thought of as free-electron-like, opposed to the polaron picture that applies to the strong-J antiferromagnetic Kondo insulator.

The inset of Fig. 4 shows a real-space snapshot of the double occupancy $\langle n_i^d \rangle$ and the density of empty sites $\langle n_i^h \rangle = 1 - \langle n_i \rangle + \langle n_i^d \rangle$ (with the ground-state value again subtracted) for $J = 12$ and a late time. The two wave packets separate in opposite directions with some spread, but little charge recombination. This demonstrates an efficient mechanism for charge separation and thus has potential relevance for solar cell devices [6].

Conclusions.—We have introduced the notion of magnetic doublons that are formed due to magnons which bind electrons in pairs. Our calculations for the Kondo lattice in one dimension have not only demonstrated their existence, but also suggest a number of highly functional properties and unconventional effects to be exploited in the future. This includes metastable superconductivity due to Bose condensation of doublons as well as quantum distillation and efficient carrier separation. Candidate materials could be the long-studied manganites [11,12], rare-earth chalcogenides or Hund's metals [14]. We also note that the Kondo model in the strong-J regime has been implemented on an ultracold lattice recently [13]. Opposed to conventional doublon excitations in the Hubbard model, magnetic doublons have a more variable dispersion which is highly sensitive to the magnetic background. The latter implies a colossal magnetoresistance effect, though curiously an inverse one, as the magnetic-doublon mobility decreases with increasing homogeneity of the spin system.

R. R. would like to thank the Japan Society for the Promotion of Science (JSPS) and the Alexander von Humboldt Foundation. Computations were partially performed at the Yukawa Institute for Theoretical Physics, Kyoto. We gratefully acknowledge the support by the Deutsche Forschungsgemeinschaft within the SFB 925 (project B5), by the Cluster of Excellence "Advanced Imaging of Matter" EXC 2056 (Project ID 390715994), as well as by JSPS KAKENHI (Grants No. JP15H05855, No. JP18H01140, No. JP18F18750, and No. JP19H01838).

*rausch.roman.72e@st.kyoto-u.ac.jp

[1] N. Strohmaier, D. Greif, R. Jördens, L. Tarruell, H. Moritz, T. Esslinger, R. Sensarma, D. Pekker, E. Altman, and E. Demler, Observation of Elastic Doublon Decay in the Fermi-Hubbard Model, Phys. Rev. Lett. **104**, 080401 (2010).

[2] R. Sensarma, D. Pekker, E. Altman, E. Demler, N. Strohmaier, D. Greif, R. Jördens, L. Tarruell, H. Moritz, and T. Esslinger, Lifetime of double occupancies in the Fermi-Hubbard model, Phys. Rev. B **82**, 224302 (2010).

[3] I. Avigo, F. Queisser, P. Zhou, M. Ligges, K. Rossnagel, R. Schützhold, and U. Bovensiepen, Doublon bottleneck in the ultrafast relaxation dynamics of hot electrons in 1T-TaS2, arXiv:1907.11677.

[4] A. Rosch, D. Rasch, B. Binz, and M. Vojta, Metastable Superfluidity of Repulsive Fermionic Atoms in Optical Lattices, Phys. Rev. Lett. **101**, 265301 (2008).

[5] T. Kaneko, T. Shirakawa, S. Sorella, and S. Yunoki, Photoinduced η Pairing in the Hubbard Model, Phys. Rev. Lett. **122**, 077002 (2019).

[6] K. A. Al-Hassanieh, F. A. Reboredo, A. E. Feiguin, I. González, and E. Dagotto, Excitons in the One-Dimensional Hubbard Model: A Real-Time Study, Phys. Rev. Lett. **100**, 166403 (2008).

[7] M. Eckstein and P. Werner, Ultrafast Separation of Photo-doped Carriers in Mott Antiferromagnets, Phys. Rev. Lett. **113**, 076405 (2014).

[8] F. Heidrich-Meisner, S. R. Manmana, M. Rigol, A. Muramatsu, A. E. Feiguin, and E. Dagotto, Quantum distillation: Dynamical generation of low-entropy states of strongly correlated fermions in an optical lattice, Phys. Rev. A **80**, 041603(R) (2009).

[9] L. Xia, L. A. Zundel, J. Carrasquilla, A. Reinhard, J. M. Wilson, M. Rigol, and D. S. Weiss, Quantum distillation and confinement of vacancies in a doublon sea, Nat. Phys. **11**, 316 (2015).

[10] S. Scherg, T. Kohlert, J. Herbrych, J. Stolpp, P. Bordia, U. Schneider, F. Heidrich-Meisner, I. Bloch, and M. Aidelsburger, Nonequilibrium Mass Transport in the 1d Fermi-Hubbard Model, Phys. Rev. Lett. **121**, 130402 (2018).

[11] K. Kubo and N. Ohata, A quantum theory of double exchange. i, J. Phys. Soc. Jpn. **33**, 21 (1972).

[12] S. Ishihara, J. Inoue, and S. Maekawa, Effective Hamiltonian in manganites: Study of the orbital and spin structures, Phys. Rev. B **55**, 8280 (1997).

[13] L. Riegger, N. Darkwah Oppong, M. Höfer, D. R. Fernandes, I. Bloch, and S. Fölling, Localized Magnetic Moments with Tunable Spin Exchange in a Gas of Ultracold Fermions, Phys. Rev. Lett. **120**, 143601 (2018).

[14] Z. P. Yin, K. Haule, and G. Kotliar, Kinetic frustration and the nature of the magnetic and paramagnetic states in iron pnictides and iron chalcogenides, Nat. Mater. **10**, 932 (2011).

[15] I. Mcculloch, A. Juozapavicius, A. Rosengren, and M. Gulácsi, Ferromagnetism in Kondo lattice models, Philos. Mag. Lett. **81**, 869 (2001).

[16] R. Rausch and M. Potthoff, Multiplons in the two-hole excitation spectra of the one-dimensional Hubbard model, New J. Phys. **18**, 023033 (2016).

[17] F. H. L. Essler, H. Frahm, F. Göhmann, A. Klümper, and V. Korepin, *The One-Dimensional Hubbard Model* (Cambridge University Press, Cambridge, England, 2005).

[18] See Supplemental Material at http://link.aps.org/supplemental/10.1103/PhysRevLett.123.216401 for supplementary calculations and derivation of the effective model.

[19] W. Nolting, S. M. Jaya, and S. Rex, Magnetic polaron in ferro- and antiferromagnetic semiconductors, Phys. Rev. B **54**, 14455 (1996).

[20] H. Tsunetsugu, M. Sigrist, and K. Ueda, The ground-state phase diagram of the one-dimensional Kondo lattice model, Rev. Mod. Phys. **69**, 809 (1997).

[21] S. Henning, P. Herrmann, and W. Nolting, Exact results on the Kondo-lattice magnetic polaron, Phys. Rev. B **86**, 085101 (2012).

[22] J. R. Schrieffer and P. A. Wolff, Relation between the Anderson and Kondo Hamiltonians, Phys. Rev. **149**, 491 (1966).

[23] S. Zhang, Pseudospin Symmetry and New Collective Modes of the Hubbard Model, Phys. Rev. Lett. **65**, 120 (1990).
[24] T. Nishino and K. Ueda, Spin- and charge-excitation gaps in the one-dimensional periodic Anderson model, Phys. Rev. B **47**, 12451 (1993).
[25] M. Potthoff, J. Braun, G. Borstel, and W. Nolting, Theory of auger electron and appearance-potential spectroscopy from solids with partially filled valence bands: Effects of valence-band–core interaction, Phys. Rev. B **47**, 12480 (1993).
[26] Y. Fukuda, Appearance potential spectroscopy (aps): Old method, but applicable to study of nano-structures, Anal. Sci. **26**, 187 (2010).
[27] A. Weiße, G. Wellein, A. Alvermann, and H. Fehske, The kernel polynomial method, Rev. Mod. Phys. **78**, 275 (2006).
[28] V. Zauner-Stauber, L. Vanderstraeten, M. T. Fishman, F. Verstraete, and J. Haegeman, Variational optimization algorithms for uniform matrix product states, Phys. Rev. B **97**, 045145 (2018).
[29] H. N. Phien, G. Vidal, and I. P. McCulloch, Infinite boundary conditions for matrix product state calculations, Phys. Rev. B **86**, 245107 (2012).
[30] J. Haegeman, C. Lubich, I. Oseledets, B. Vandereycken, and F. Verstraete, Unifying time evolution and optimization with matrix product states, Phys. Rev. B **94**, 165116 (2016).
[31] F. Hofmann and M. Potthoff, Doublon dynamics in the extended Fermi-Hubbard model, Phys. Rev. B **85**, 205127 (2012).
[32] R. Rausch and M. Potthoff, Filling-dependent doublon dynamics in the one-dimensional Hubbard model, Phys. Rev. B **95**, 045152 (2017).